



Taylor & Francis
Taylor & Francis Group



Multivariate Time Series Projections of Parameterized Age-Specific Fertility Rates

Author(s): Patrick A. Thompson, William R. Bell, John F. Long and Robert B. Miller

Source: *Journal of the American Statistical Association*, Sep., 1989, Vol. 84, No. 407 (Sep., 1989), pp. 689-699

Published by: Taylor & Francis, Ltd. on behalf of the American Statistical Association

Stable URL: <https://www.jstor.org/stable/2289650>

JSTOR is a not-for-profit service that helps scholars, researchers, and students discover, use, and build upon a wide range of content in a trusted digital archive. We use information technology and tools to increase productivity and facilitate new forms of scholarship. For more information about JSTOR, please contact support@jstor.org.

Your use of the JSTOR archive indicates your acceptance of the Terms & Conditions of Use, available at <https://about.jstor.org/terms>



JSTOR

Taylor & Francis, Ltd. and American Statistical Association are collaborating with JSTOR to digitize, preserve and extend access to *Journal of the American Statistical Association*

Multivariate Time Series Projections of Parameterized Age-Specific Fertility Rates

PATRICK A. THOMPSON, WILLIAM R. BELL, JOHN F. LONG, and ROBERT B. MILLER*

Projection of individual age-specific fertility rates is a forecasting problem of high dimension. We solve this dimensionality problem by using parametric curves to approximate the annual age-specific rates and a multivariate time series model to forecast the curve parameters. These yield forecasts of future fertility curves, which are then used to compute age-specific fertility rate forecasts. This reduces the dimensionality of the forecasting problem and also guarantees that long-run projections of age-specific fertility rates will exhibit a smooth shape across age similar to historical data. Short-term projections are improved by also using simple techniques to forecast the deviations of the fitted curves from the actual rates. The article applies this approach to age-specific fertility data for U.S. white women from 1921–1984. The resulting forecasts are examined, and the multivariate model is used to investigate possible relations between the curve parameters, expressed as the total fertility rate, the mean age of childbearing, and the standard deviation of age at childbearing. The only strong relationship found is the contemporaneous relationship between the mean and standard deviation of age at childbearing. A variation of this approach, in conjunction with traditional demographic judgment, was used in a recent set of U.S. Census Bureau population projections. We discuss this implementation and compare the Census Bureau projections with those produced directly from the model presented here.

KEY WORDS: Fertility projection; Multivariate ARIMA models.

1. INTRODUCTION

Fertility projections are a vital part of any system for predicting the size and structure of a population. Under the cohort-component projection method, total births are forecast by multiplying age-specific fertility rates by the number of females at each age. In this approach, the projected number of women at each age has a major impact on the projected number of births, but is the most predictable element of the process. At the time a projection is made, most of the women who will bear children over the next 25 years are already alive.

Early projections by the U.S. Bureau of the Census held age-specific fertility rates constant and let total future births vary only with changes in the number of women at each age (Whelpton 1947). Over time, however, the age-specific rates have been quite volatile. More recent projections of fertility rates interpolated between the last year of observed data and an assumed ultimate schedule of

fertility (U.S. Bureau of the Census 1984). Alternative high and low ultimate fertility levels were set judgmentally, and new interpolations produced alternative fertility projections. This technique relied heavily on substantive judgment in setting realistic assumptions of future fertility schedules, and these assumptions varied from projection to projection.

We develop a time series modeling approach to forecasting age-specific fertility rates. In doing this, we must first decide whether to analyze data structured by period (calendar years) or by cohorts (years mothers were born). Period-based approaches were largely replaced by cohort methods in the 1960s when projections were heavily based on surveys of birth expectations. Recent arguments for a period approach emphasize the effects of economic conditions, which simultaneously affect the fertility of women at all childbearing ages. Some efforts (De Beer 1985; Wilkens 1984) combine both approaches.

Without directly entering the period-cohort controversy, we perform our analysis on a period basis for essentially practical reasons. The use of age-specific data on a cohort basis creates massive incomplete data problems, since a cohort fertility record is not complete for some 30 years after its first births are observed. Moreover, cohort fertility rates do not follow the smooth patterns across age evidenced in period fertility rates. Our goal is to improve the short-term fertility forecasts in the national population projections. Period analysis emphasizes the short-term trends in fertility that simultaneously affect all ages. Cohort analysis appears more important over longer horizons. Thus, in this article, our emphasis is on projecting age-specific fertility on a period basis.

We follow the time series tradition in our approach to forecasting age-specific fertility rates and follow the demographic cohort-component tradition in multiplying these by projections of the age-specific female population

* Patrick A. Thompson is Professor of Decision and Information Sciences, College of Business Administration, University of Florida, Gainesville, FL 32611. William R. Bell is Mathematical Statistician, Statistical Research Division, Bureau of the Census, U.S. Department of Commerce, Washington, DC 20233. John F. Long is Chief, Population Projections Branch, Bureau of the Census, U.S. Department of Commerce, Washington, DC 20233. Robert B. Miller is Professor of Business and Statistics, University of Wisconsin, Madison, WI 53706. This article is based on work supported by National Science Foundation (NSF) Grant SES 81-22051 ("Research to Improve the Government-Generated Social Science Data Base"). The research was partially conducted at the Bureau of the Census while two of the authors (Thompson and Miller) were participants in the American Statistical Association/Census Bureau Research Program, supported by the Census Bureau and through the NSF grant. Any opinions, findings, conclusions, and recommendations expressed here are those of the authors and do not necessarily reflect the views of the NSF or the Census Bureau. Additional funding was provided by Ohio State University Seed Money Grant 221772 in 1985 and by the Census Bureau through Ohio State University Research Foundation Grant RF-717887 in 1985–1986. Thompson was in the Department of Management Sciences at Ohio State University from 1984 to 1989. The authors thank Gregory Spenser (Population Division, U.S. Bureau of the Census) for supplying data and assistance in the cohort analysis, Marian Pugh (Statistical Research Division, Census Bureau) for assistance with the graphics, and three anonymous referees for helpful comments on an earlier version of this article.

to yield total fertility forecasts. The former is more statistically rigorous in modeling variability in fertility, and the latter takes advantage of the predictable size and age structure of the female population. The benefits of combining the major traditions of population projection were outlined by Long (1984) and Land (1986). In practice, we have also combined short-term time series forecasts of fertility rates with long-term projections of completed cohort fertility determined through demographic judgment.

Several authors have applied time series methods by themselves, using autoregressive integrated moving average (ARIMA) models. McDonald (1979, 1981) and Saboia (1977) forecast total births, efforts that yielded some insights into the use of time series techniques on fertility, but ignored the advantage of using cohort-component methods (Long 1981). This omission was partially remedied by Lee (1974, 1975) and Carter and Lee (1986), who forecast series measuring fertility within a standardized age structure. If, however, the age pattern of fertility changes, it can only be captured by accounting for fertility by single years of age.

Dimensionality is the major problem faced in using time series methods to forecast age-specific fertility. Data for women of ages 14–45 yield 32 time series to be modeled. This is a large number of series even for univariate approaches, and practicality would likely demand consideration of only a few simple models. A second potential problem is inconsistency of the age-specific forecasts. Using separate univariate models for 32 fertility rates, the forecasts at various ages might follow different trends, so the ultimate schedule of fertility across age may not make sense. We can expect that future fertility rates will be smooth functions of age with a shape similar to historical patterns; constraints on the univariate models may be required to achieve this structure.

The system is far too large for general multivariate models; a full AR(1) model would have 1,024 (32×32) autoregressive parameters. An alternative is a multivariate model with a simplified structure, such as the cohort ARIMA (CARIMA) model of De Beer (1985). The CARIMA approach lets the fertility rate at a given age and cohort depend on the rates at prior ages in the same cohort and on rates for the same age in prior cohorts, using the same model for all cohort–age combinations. This constraint was necessary in De Beer's application with limited time series data, but seems overly restrictive with our 64 years of data.

The approach we adopt uses a different type of simplification to address the problems of dimensionality and consistency while retaining the advantages of ARIMA models for short-term forecasting. Section 2 shows how each annual set of historical fertility rates can be fit by a curve with only a few parameters. Section 3 indicates how the curve parameters can be modeled through multivariate time series techniques. In Section 4, we forecast the parameters to generate model curves of future fertility rates. Section 5 discusses implementation in the most recent set of national population projections (U.S. Bureau of the Census 1988) and compares our model forecasts to the

fertility projections actually used, which were produced through a combination of time series and demographic techniques.

The advantages of this method are that it reduces the dimension of the problem from 32 to 4 (the number of curve parameters), and the curves force even long-term fertility projections to exhibit the same smooth distribution across age as historical data. The technique, however, has one drawback: It forecasts not the future rates themselves, but curves that approximate the rates. In its basic form it assumes that the error in approximating the rates is negligible for forecast purposes. Although this is true for long-term projections, it is not so in the short term (1–5 years ahead). We deal with this in Section 4 by using simple models to forecast the *biases*, the deviations of the fitted curves from the actual rates. This greatly improves the accuracy of short-term forecasts while still accomplishing the goals of dimensionality reduction and long-term consistency. Most of the effort is focused on modeling and forecasting the curve parameters.

2. APPROXIMATING PERIOD FERTILITY RATES WITH GAMMA CURVES

Hoem, Madsen, Nielsen, and Ohlsen (1981) fit several curves to Danish age-specific fertility rates, obtaining equally good fits with the Coale–Trussell (1974) function and gamma density. (Ten-parameter cubic splines yielded even better fits, but have too many parameters for our purposes.) The Coale–Trussell function is somewhat complicated, involving tables of two age-specific functions and the integral of what Rogers (1986) called a double exponential function. Rogers suggested direct use of the double exponential function as a simpler alternative. We use the gamma curve, scaled and shifted, because of its simplicity and good fit relative to other curves considered.

Our approach—fitting a curve to fertility rates and forecasting its parameters—can certainly be used with curves other than the gamma (the double exponential curve yields comparable fits). The choice is not critical for forecasting purposes, since no parametric curve is likely to be immune from the short-term bias problem. We view the curve as a device for dimensionality reduction, and we do not propose using it as a “model” for estimating age-specific fertility rates in populations for which only summary fertility data are available. Our data contain full age-specific detail and are obtained from the essentially complete reporting of births in the Vital Statistics Registration System, so there is no sampling error.

The historical fertility data base we use consists of age-specific fertility rates of United States white women from 1921 through 1984 [Heuser (1976) and more recent unpublished data]. These are recorded for women of ages 14 and under, single ages of 15 through 44, and 45 and over, yielding an initial data matrix of 64 observations on 32 concurrent time series. Figure 1 shows the period fertility rates for 1927, 1957, and 1977. Although total fertility was markedly different in these years, the three sets of rates have a similar smooth shape over age. Figure 2 shows

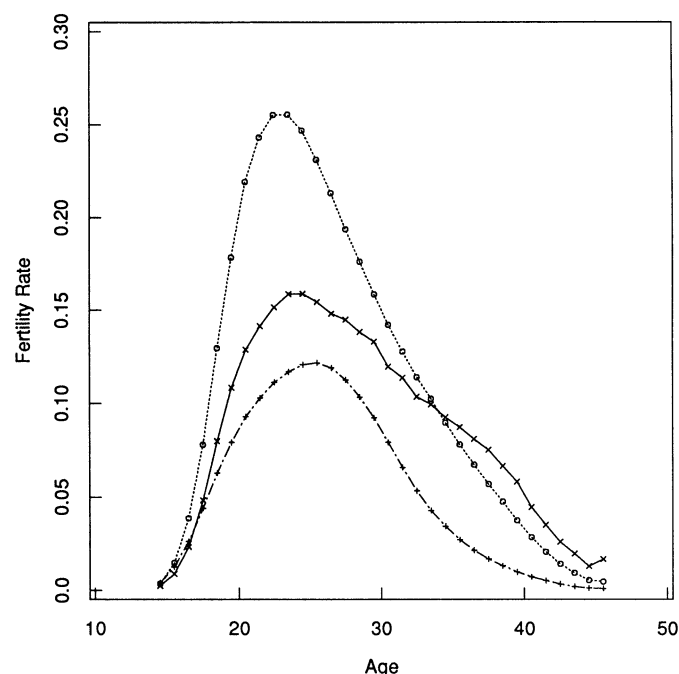


Figure 1. Period Age-Specific Fertility Rates for U.S. White Women for Three Years: 1972 (\times), 1957 (o), and 1977 (+). Total fertility differs and the age-specific pattern shifts over time, but the period fertility rates have a similar smooth shape across age that is well-approximated by a scaled and shifted gamma density. The largest deviations from this shape occur in the early years of data (e.g., 1927), which are the least important for forecasting. The rates are plotted at the mother's age at last birthday plus .5.

age-specific fertility rates for the 1902, 1932, and 1952 birth cohorts, which reach age 25 (a peak childbearing age) in 1927, 1957, and 1977, respectively. In addition to illustrating the incomplete data problems when analyzing data on a cohort basis, Figure 2 shows that rates for different cohorts do not follow the same smooth shape across age. The problems are most pronounced in recent cohorts, for example, the 1952 cohort.

To approximate the fertility rates each year, we fit a shifted gamma probability density function to the scaled age-specific rates, using the parametric form

$$\gamma_i = \frac{1}{\Gamma(\alpha)\beta^\alpha} (i - A_0)^{\alpha-1} \exp\{-(i - A_0)/\beta\}, \quad i \geq A_0, \quad (2.1)$$

where $\Gamma(\alpha) = \int_0^\infty u^{\alpha-1} \exp\{-u\} du$. This density has probability starting at the point A_0 , expected value $A_0 + \alpha\beta$, and variance $\alpha\beta^2$. Since the gamma curve integrates to 1, in fitting it we rescale the age-specific fertility rates so that they sum to unity in each year. Let F_{it} denote the fertility rate per woman of age i in year t , define the total fertility rate (TFR) in year t as

$$\text{TFR}_t = \sum_{i=14}^{45} F_{it}, \quad (2.2)$$

and compute the “relative” fertility rate to women age i in year t as

$$R_{it} = F_{it}/\text{TFR}_t, \quad i = 14, 15, \dots, 45, \quad t = 1921, \dots, 1984.$$

R_{it} is the proportion of births in year t that occur to mothers of age i .

Now let γ_{it} denote the height, at age $i > A_0$, of a shifted gamma curve with parameters A_0 , α_t , and β_t . We fit the curve to the R_{it} in each year t by minimizing the sum of weighted squared errors:

$$\text{WSSE}_t = \sum_{i=14}^{45} [w_i(R_{it} - \gamma_{it})]^2, \quad (2.3)$$

where w_i is the weight for age i . The parameter values for α and β are determined through a derivative-based non-linear least squares procedure operating conditional on values of A_0 . Values for the starting point of the curve, A_0 , are obtained from a one-dimensional search constrained to the region $0 \leq A_0 \leq 14$. In practice, the values γ_{it} are computed at ages 14.5, \dots , 45.5, since fertility is recorded at the mother's last birthday.

Since a main reason for forecasting fertility rates is to forecast total births, we use the weights to give more emphasis to ages with high fertility. In recent years most births (80%–85%) are to women aged 18 through 32. We use the simple scheme $w_i = 4$, $18 \leq i \leq 32$, and $w_i = 1$ otherwise. Sensitivity analysis, examining the response of the gamma parameters to changes in the w_i , shows that the exact weight used for ages 18–32 has much less impact than the fact that these ages are singled out for special treatment. For example, α_{1982} and β_{1982} change only one unit in their third significant digits when weights of 2 through 6 are used.

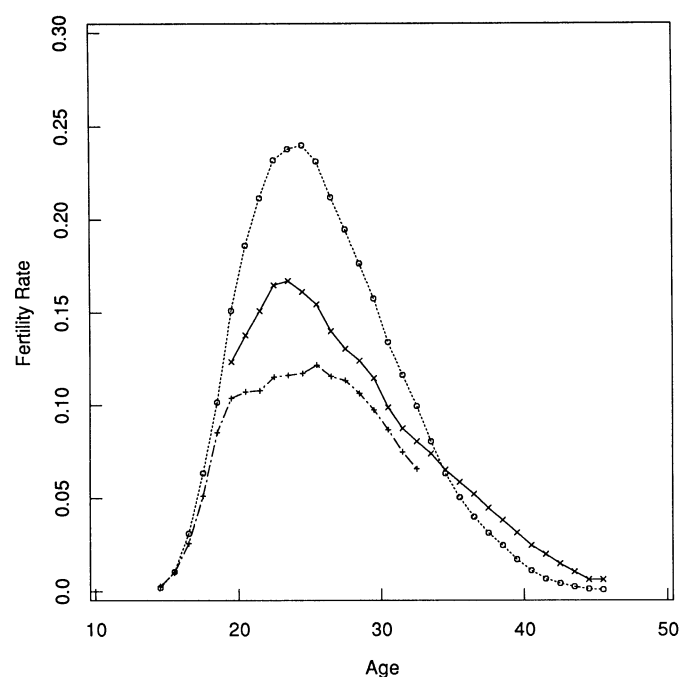


Figure 2. Cohort Age-Specific Fertility Rates for U.S. White Women for Three Cohorts: 1902 (\times), 1932 (o), and 1952 (+). Since we use data for 1921–1984, the 1902 cohort is incomplete at ages 14–19, and the 1952 cohort is incomplete at ages 33–45. In contrast to period rates, cohort rates do not follow such similar smooth shapes across age. Large deviations from a common smooth shape occur in recent cohorts, which are the most important for forecasting. The fertility rates for recent cohorts (e.g., 1952) are relatively flat for ages 19–30. The rates are plotted at the mother's age at last birthday plus .5.

This weighting scheme disagrees with that of Rogers (1986), who fit curves via a chi-squared goodness-of-fit criterion. Although not stated explicitly, Rogers apparently minimized $\sum(O_i - E_i)^2/O_i$, where O_i and E_i denote, respectively, the observed rate and the curve value at age i ; in our case these are R_{it} and γ_{it} . This approach gives more weight to the ages with the *lowest* fertility rates (smallest O_i). Our weighting scheme places more weight on the fit at ages with *high* fertility, so the curves yield better approximations to total births while not ignoring the fit at other ages. Different individuals are, of course, free to choose different weights reflecting their own "loss functions."

The curve fits are summarized in Figure 3, which traces the curve parameters over time. Apart from the years affected by World War II, these traces are stable through 1968, even though total fertility varies considerably over this period. During the 1970s, however, the parameters shift rapidly to new levels. The shift in the pattern of fertility is illustrated by Figure 4, where we show the gamma curves for 1927 and 1977. In the early part of our data base, there is more fertility to older women; later, fertility is concentrated to women in their twenties and the gamma curves have more symmetric shapes. In recent years, the curves also fit much better, an important consideration since ARIMA model forecasts reflect behavior nearest to the forecast origin.

Some comments on the behavior of A_0 are in order. Through 1968, WSSE (2.3) was usually minimized at $A_0 = 14$ (this upper limit was imposed so the gamma curve would yield an ordinate at age 14). In recent years, as α and β shift to make the curves more symmetric, A_0 decreases and WSSE is rather insensitive to values of A_0 from 0 through negative numbers large in magnitude. To simplify the least squares problem, a lower limit of 0 was used with little sacrifice in quality of fit. Since A_{0t} has almost a two-point distribution over time, however, it is ill-suited for modeling. It seems reasonable to treat A_{0t} as

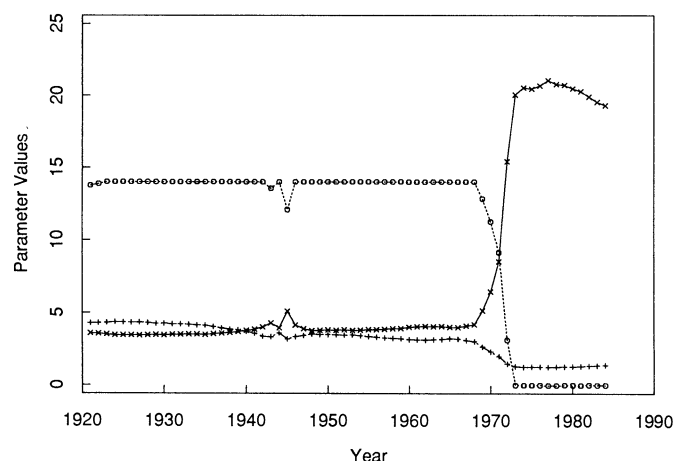


Figure 3. Parameters of Gamma Curves Fit to Relative Fertility Rates of U.S. White Women, 1921–1984: A_{0t} (o), α_t (x), and β_t (+). Except for years affected by World War II (1942–1947), the parameters remain relatively stable through 1968, after which they shift rapidly to new levels. In fitting the gamma curves, values of the endpoint parameter A_{0t} were constrained to the interval $[0, 14]$ (see text).

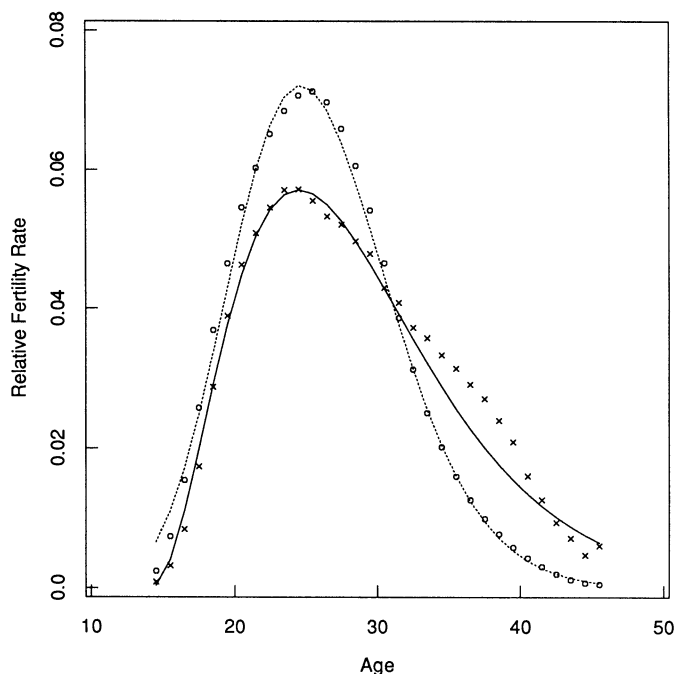


Figure 4. Two Fitted Relative Fertility Curves. We exhibit the fitted curves from 1927 (—) and 1977 (---), which have, respectively, the smallest and largest α values. The three adjustable parameters (A_0 , α , and β) allow the gamma curves to approximate a variety of age-specific fertility patterns. The observed relative fertility rates in 1927 (x) and 1977 (o) are also shown. In general, the fitted curves provide good overall approximations of the data. Note that the approximation is better in the latter year.

deterministic: We project, rather than model and forecast, A_0 at its most recent level of 0.

In modeling the gamma system over time, we first transform the α and β parameters. Since the gamma density (2.1) has expected value $A_0 + \alpha\beta$ and variance $\alpha\beta^2$, we form the new series:

$$\text{MACB}_t = A_{0t} + \alpha_t\beta_t, \quad \text{SDACB}_t = \beta_t \cdot (\alpha_t)^{1/2}. \quad (2.4)$$

These are the mean age and standard deviation of age at childbearing, computed from the gamma density. MACB and SDACB have more stable traces over time: Figures 5 and 6 show that these series do not have the abrupt shifts in level that α and β display in Figure 3. The new series also have more meaningful demographic interpretations, which facilitates combination of short-term forecasts of MACB and SDACB with analogous quantities projected long term by demographic judgment.

3. TIME SERIES MODELING OF CURVE PARAMETERS

One of the primary questions addressed in setting ultimate fertility schedules by demographic judgment is whether the level of fertility affects the distribution by age. In previous Census Bureau projections the level of fertility was assumed independent of the age-specific distribution, although there was some speculation about possible relationships. For the current work, we wanted to examine empirical evidence on the relationships and use this information in both the long-term and short-term fertility

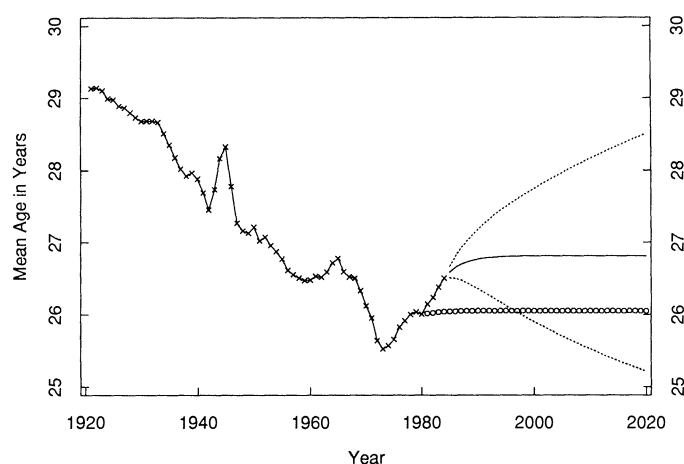


Figure 5. Mean Age of Childbearing From Gamma Curve: Data (\times) and Forecasts. Forecasts for $M_t = \ln(\text{MACB}_t)$ use Model (3.1) with estimated parameters. Exponentiation provides point forecasts from 1980 (o) and 1984 (—), and 67% interval limits from 1984 (---) for MACB_t . Model parameters are estimated using data up through the forecast origin years (1980 or 1984).

projections. To perform this examination, we model the joint behavior of the series over time through a multivariate ARIMA model for TFR, MACB, and SDACB.

Prior to developing this model, we take two preparatory steps. First, we transform TFR_t , MACB_t , and SDACB_t to $T_t = \ln(\text{TFR}_t)$, $M_t = \ln(\text{MACB}_t)$, and $S_t = \ln(\text{SDACB}_t)$. Since negative birth rates are impossible, TFR is transformed to prevent its lower forecast limit from going below 0. Taking logarithms does not materially affect the modeling of MACB and SDACB, since the transformation is nearly linear over the range of those series. Transforming all three series helps interpretation of the models, however, since any additive relationships among T , M , and S may be interpreted as multiplicative relations between TFR, MACB, and SDACB.

A second step adjusts the log series for the effects of World War II on fertility (Figs. 3 and 5–7 all display un-

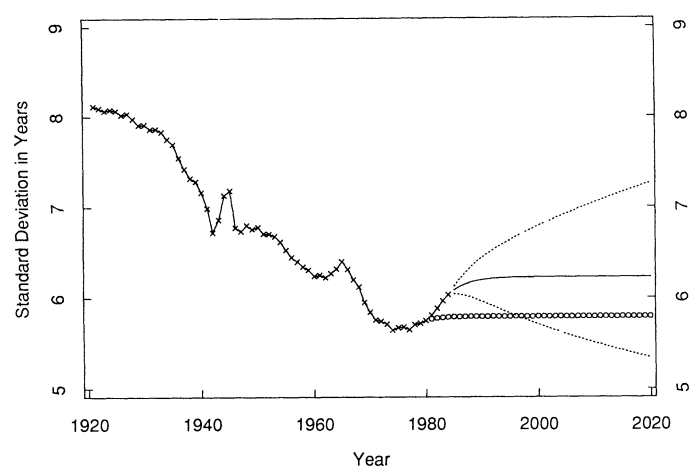


Figure 6. Standard Deviation of Age at Childbearing From Gamma Curve: Data (\times) and Forecasts. Forecasts for $S_t = \ln(\text{SDACB}_t)$ use Model (3.1) with estimated parameters. Exponentiation provides point forecasts from 1980 (o) and 1984 (—), and 67% interval limits from 1984 (---) for SDACB_t . Model parameters are estimated using data up through the forecast origin years (1980 or 1984).

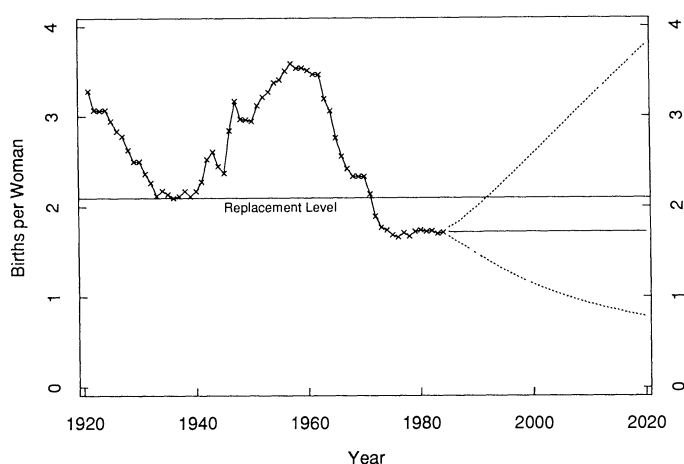


Figure 7. Total Fertility Rate per U.S. White Woman: Data (\times) and Forecasts. Forecasts for $T_t = \ln(\text{TFR}_t)$ use Model (3.1) with estimated parameters. Exponentiation provides point forecasts from 1984 (—) and 67% interval limits (---) for TFR_t . Notice the asymmetry of the resulting forecast intervals. Forecasts from 1980 are not shown, since they would almost coincide with the 1981–1984 data and the 1984 point forecasts. Also shown for reference is a line at 2.1, the “replacement level” for TFR (see text).

usual behavior during 1942–1947). We estimate these effects, which are inconsistent with a pure ARIMA model, via univariate models that include indicator regression variables for the years 1942–1947 and ARIMA errors. These have the form

$$y_t = \beta_1 I_{42t} + \dots + \beta_6 I_{47t} + [\theta(B)/\phi(B)\delta(B)]a_t,$$

where I_{42t}, \dots, I_{47t} are war-year indicator variables; β_1, \dots, β_6 are parameters; $\theta(B)$, $\phi(B)$, and $\delta(B)$ are the moving average, autoregressive, and differencing operators in the backshift operator B ; y_t is the particular series being modeled; and a_t is a sequence of iid $N(0, \sigma^2)$ random variables (white noise). The ARIMA structure is identified following the scheme suggested by Bell and Hillmer (1983) for models of this type. The resulting models have a differencing order of 1 for all three series, with an AR(3) model for ∇T_t and AR(2) models for ∇M_t and ∇S_t ($\nabla = 1 - B$ denotes first difference). Further details are given in Bell, Long, Miller, and Thompson (1988).

3.1 The Multivariate Time Series Model

The war-year effects estimated previously are subtracted (e.g., by taking $T_t - \hat{\beta}_1 I_{42t} - \dots - \hat{\beta}_6 I_{47t}$) and the resulting series first differenced. Henceforth, let T_t , M_t , and S_t denote the war-year adjusted series, and let $\nabla Y_t = (\nabla T_t, \nabla M_t, \nabla S_t)'$ denote the differenced vector series. Multivariate identification proceeds as in Tiao and Box (1981) by examining cross-correlation matrices and stepwise AR fits. These suggest a pure AR model: stepwise AR tests (Table 1) truncate, but the cross-correlation matrices (Fig. 8) do not.

Although the overall statistics suggest an AR(1) model, in the AR(3) fit the (1, 1) element [corresponding to ∇T_t , which has an AR(3) univariate model] of the third AR parameter matrix is significant. No other parameter estimates in the second- and third-order matrices of the full

Table 1. Multivariate Model Identification Exhibits:
Stepwise Autoregressive Fits

Maximum AR lag	$ \Sigma_j \times 10^{13}$	χ^2 test	AIC
0	9.47		-1,578
1	2.61	59.9	-1,634
2	2.01	11.4	-1,630
3	1.71	6.6	-1,622
4	1.32	9.6	-1,618
5	1.22	2.7	-1,605
6	1.08	3.9	-1,594

NOTE: The asymptotic χ^2 test statistic of $\Phi_j = 0$ in an AR(j) fit is $-(49.5 - 3j)\ln(|\Sigma_j|/|\Sigma_{j-1}|)$, starting from $|\Sigma_0|$. With 9 df, the 5% critical value is 16.9. AIC denotes the Akaike information criterion, computed here as $57 \ln|\Sigma| + 2(9j)$ for the lag j fit. Akaike (1973) suggested picking the AR model for which this criterion is minimized.

AR(3) fit exceed twice their standard errors. Rather than use a full AR(3) model with 27 parameters (not counting the residual variances and covariances) we consider a restricted model:

$$\nabla Y_t = \Phi_1 \nabla Y_{t-1} + \Phi_2 \nabla Y_{t-2} + \Phi_3 \nabla Y_{t-3} + a_t, \quad (3.1)$$

where Φ_1 is an unconstrained 3-by-3 parameter matrix, Φ_2 and Φ_3 have all the elements except those at the (1, 1) locations constrained to 0, and $a_t = (a_{1t}, a_{2t}, a_{3t})'$ is a vector white noise series with covariance matrix Σ . Estimation by conditional likelihood yields

$$\hat{\Phi}_1 = \begin{bmatrix} .458 & 2.754 & -1.027 \\ .014 & .337 & .140 \\ .045 & .264 & .632 \end{bmatrix}$$

with standard errors

$$\begin{bmatrix} .122 & 1.465 & .597 \\ .010 & .152 & .060 \\ .023 & .353 & .139 \end{bmatrix}.$$

$\hat{\Phi}_2(1, 1) = .026$ with standard error .132, $\hat{\Phi}_3(1, 1) = .324$ with standard error .117, and

$$\hat{\Sigma} = 10^{-4} \times \begin{bmatrix} 8.190 & & \\ -.040 & .094 & \\ -.639 & .133 & .509 \end{bmatrix}.$$

Diagnostic checks reveal no obvious inadequacies with the exception of some outliers in the residuals of T_t and M_t , which will not materially affect the forecasts of these series. Details on outlier adjustment and some alternative models are in Bell et al. (1988).

3.2 Relations Among the Curve Parameters

An important feature of this model is that it allows us to examine relations between TFR and the mean age and standard deviation of age at childbearing. Model (3.1) allows for dynamic effects of the variables T_t , M_t , and S_t on each other through the off-diagonal elements of Φ_1 and contemporaneous effects through the off-diagonal elements of Σ . The t statistics for $\hat{\Phi}_1$ and the residual

correlation matrix, \hat{C} , corresponding to $\hat{\Sigma}$, are the following:

$$t(\hat{\Phi}_1): \begin{bmatrix} 3.8 & 1.9 & -1.7 \\ 1.4 & 2.2 & 2.3 \\ 2.0 & .7 & 4.5 \end{bmatrix},$$

$$\hat{C} = \begin{bmatrix} 1.00 & & \\ -.05 & 1.00 & \\ -.31 & .61 & 1.00 \end{bmatrix}. \quad (3.2)$$

The off-diagonal elements of Φ_1 are at most marginally significant, suggesting that the dynamic relationships are not strong. A more formal check is obtained by fitting a model with Φ_1 restricted to be diagonal; this amounts to fitting three univariate models jointly with a correlated error structure. The residual covariance matrix for this model was

$$\hat{\Sigma}_2 = 10^{-4} \times \begin{bmatrix} 8.659 & & \\ -.115 & .107 & \\ -.656 & .151 & .566 \end{bmatrix}.$$

An asymptotic $\chi^2(6)$ test of the restrictions on Φ_1 (6 df for the off-diagonal elements) is obtained using $Q = -m \cdot \ln\{|\hat{\Sigma}|/|\hat{\Sigma}_2|\}$ (see Hannan 1970, pp. 339–341). The choice of the $O(n)$ multiplier m is not obvious; we followed Rao (1965, chap. 8) and used $m = (51 + 2) - .5(3 + 2 + 1) = 50$, where 3 is the dimension (number of equations), 2 is the number of parameters constrained in each equation, and 51 is the residual df in each equation of the full model [64 observations, less 4 lost to differencing and AR order, less 6 war-year and 3 AR(1) parameters estimated, but ignoring the estimation of the lag 2 and 3 parameters in the T_t equation]. This yields $Q = 15.8$, which is at about the 98.5 percentile of the $\chi^2(6)$ distribution, suggesting that the dynamic relationships are marginally significant, but not strong.

If the Φ_1 matrix is lower triangular (possibly after reordering Y_t), the relationships modeled by (3.1) may be restated in an equivalent transfer function form (Tiao and Box 1981, pp. 802–803). In (3.1), the contemporaneous relationships among the variables T_t , M_t , and S_t are modeled implicitly through Σ . Transfer function models may contain explicit statements of contemporaneous effects, and this aids the empirical examination of the relationships between fertility level (TFR) and distribution by age (MACB and SDACB).

The t statistics in (3.2) imply that no individual dynamic

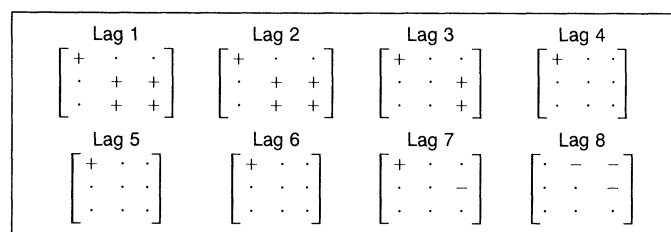


Figure 8. Multivariate Model Identification Exhibits: Simplified Cross-Correlation Matrices, Lags 1–8. + indicates a T-ratio ≥ 2 , - indicates a T-ratio ≤ -2 , and . indicates $-2 < T < 2$.

relationship is strong, thus argue neither for nor against any particular lower triangular structure for Φ_1 . We experimented with several transfer function models and, not surprisingly, found dynamic effects in them at most marginally significant. If we accept the hypothesis of no dynamic effects, then we can use a simple transfer function model where the variables have only concurrent dependence and can be entered in any order. Modeling variables in the order $T_t \rightarrow M_t \rightarrow S_t$ yields (standard errors in parentheses)

$$\begin{aligned} T_t &= a_{1t}/(1 - .54B - .01B^2 + .24B^3)(1 - B) \\ &\quad (.13) \quad (.14) \quad (.12) \\ M_t &= -.0140T_t + a_{2t}/(1 - .53B - .20B^2)(1 - B) \\ &\quad (.0134) \quad (.13) \quad (.13) \\ S_t &= -.061T_t + 1.18M_t \\ &\quad (.025) \quad (.24) \\ &\quad + a_{3t}/(1 - .44B - .29B^2)(1 - B). \quad (3.3) \\ &\quad (.13) \quad (.12) \end{aligned}$$

The only strong contemporaneous relationship is that between M_t and S_t , with that between T_t and S_t marginally significant. This provides a significance check on what we would also infer from the correlation matrix \hat{C} in (3.2).

In the absence of time series data on his curve parameters, Rogers (1986) suggested a regression approach to projection. In our case this implies projecting T_t independently (either by judgment or using models), regressing M_t and S_t on T_t , and using the regression relations to develop M_t and S_t projections from the T_t projections. The weak relationships of T_t to M_t and S_t in (3.3) show that this would be a poor approach with the gamma curve. Since TFR refers to the overall level of fertility and MACB and SDACB refer to the shape of the curve, the shape of the fertility curve appears to depend little on the level. Thus we expect that Rogers's approach would also not work well with other curves applied to our data, and we would recommend caution in applying it to other fertility data sets.

4. FORECASTS AND BIAS ADJUSTMENT

We use (3.1) to forecast due to the marginal significance of the dynamic relationships. Since individual dynamic relationships are not strong, however, use of diagonal Φ_1 or transfer function models should not yield greatly different results. To use (3.1) in forecasting, we incorporate the differencing into the AR operator and write

$$Y_t = \Pi_1 Y_{t-1} + \Pi_2 Y_{t-2} + \Pi_3 Y_{t-3} + \Pi_4 Y_{t-4} + a_t, \quad (4.1)$$

where $\Pi_1 = I + \Phi_1$, $\Pi_2 = \Phi_2 - \Phi_1$, $\Pi_3 = \Phi_3 - \Phi_2$, and $\Pi_4 = -\Phi_3$. In forecasting, we do not need to account explicitly for the war-year variables, since they are all 0 over the forecast horizon.

Forecasts $\hat{Y}_n(k)$ of $Y_{n+k} = (T_{n+k}, M_{n+k}, S_{n+k})'$ from any origin n are computed recursively for $k = 1, 2, \dots$ from

$$\begin{aligned} \hat{Y}_n(k) &= \Pi_1 \hat{Y}_n(k-1) + \Pi_2 \hat{Y}_n(k-2) \\ &\quad + \Pi_3 \hat{Y}_n(k-3) + \Pi_4 \hat{Y}_n(k-4), \quad (4.2) \end{aligned}$$

where $\hat{Y}_n(j) = Y_{n+j}$ for $j \leq 0$. The variance of the k -step-ahead forecast error, $Y_{n+k} - \hat{Y}_n(k)$, is given by

$$V(k) = I + \psi_1 \Sigma \psi_1' + \dots + \psi_{k-1} \Sigma \psi_{k-1}', \quad (4.3)$$

where the ψ_j matrices are obtained by equating coefficients on B^j in $(I + \psi_1 B + \psi_2 B^2 + \dots)(I - \Pi_1 B - \Pi_2 B^2 - \Pi_3 B^3 - \Pi_4 B^4) = I$.

The diagonal elements $\{v_{ii}(k); i = 1, 2, 3\}$ of $V(k)$ are the variances of the forecast errors and may be used to produce forecast intervals for T_t , M_t , and S_t , assuming normality. For example, $\hat{T}_n(k) \pm h(v_{11}(k))^{1/2}$ provides an approximate 67% ($h = 1$) or 95% ($h = 2$) forecast interval for T_{n+k} . Exponentiating the point forecasts and interval limits for T_t , M_t , and S_t yields point and interval forecasts for TFR, MACB, and SDACB. In practice, we use the estimates of Φ_1 , Φ_2 , Φ_3 , and Σ in (4.1)–(4.3).

Figures 5–7 show point and 67% interval forecasts from origin 1984 for TFR, MACB, and SDACB, and point forecasts from 1980 for MACB and SDACB. For the latter, Model (3.1) was reestimated using only data through 1980. (The 1980-origin point forecasts for TFR are not shown because they would almost coincide on the graph with the 1981–1984 data and 1984 forecasts.) These forecasts are determined primarily by the last two years of data, since (3.1) is almost an AR(1) model in the first difference [only the (1, 1) elements of Π_3 and Π_4 in (4.2) are nonzero]. This results in very flat point forecasts from 1980, since the change from 1979 to 1980 is small for all three series. The sharp increase in MACB and SDACB from 1980 through 1984 produces MACB and SDACB forecasts from 1984 that increase before leveling off. The long-term point forecasts all level off because of the first differencing and absence of a constant term in (3.1). This behavior is convenient for long-term forecasting, since it facilitates comparison with traditional long-term judgmental forecasts made by specifying an ultimate level for the series being forecast, as discussed in Section 1. Models with other degrees of differencing or a constant term would exhibit different long-run forecast behavior.

The forecast intervals in Figures 5–7 show that there is considerable uncertainty associated with long-term forecasts for all three series. Focusing on TFR, Figure 7 indicates what demographers refer to as the replacement level of TFR, which is currently approximately 2.1 in the United States. If TFR remains constant at this level, with no change to mortality and relative fertility rates and zero net migration, then population size remains approximately constant. TFR for U.S. white women dropped below replacement level for the first time in 1972 and has since remained well below that level. Although the point forecasts for TFR stay below 2.1, the forecast limits show considerable uncertainty in how long TFR will remain below replacement level. For the 1984-origin forecasts, the upper 67% and 95% limits exceed 2.1 in 1992 and 1988, respectively.

The forecasts of TFR, MACB, and SDACB, along with the projection of A_0 at 0, may be used to forecast future gamma fertility curves. These are forecasts of the curves

that will be fit to the future data when they become available. To forecast the actual age-specific fertility rates, we also want to forecast the deviations of the rates from the curve and include this *bias adjustment* in the computation.

The relative fertility rates, R_{it} , are defined in Section 2. Let γ_{it} denote the ordinate of (2.1), for age i in year t ; we use the relation

$$F_{it} = \text{TFR}_i(\gamma_{it} + b_{it}), \quad i = 14, \dots, 45, \quad (4.4)$$

where $b_{it} = R_{it} - \gamma_{it}$ is the bias, to produce bias-adjusted forecasts.

The autocorrelation functions for the 32 age-specific bias series indicate that all series appear to need differencing. For the most part, autocorrelation remaining after a first difference is applied is not strong. For simplicity, we use the random walk model $\nabla b_{it} = \varepsilon_{it}$, with ε_{it} white noise, for all of the bias series. The forecast of $b_{i,n+k}$ is then just $\hat{b}_{in}(k) = b_{in}$; that is, the biases are all forecast to remain constant at their values in the forecast origin year. Projections of $A_{0,n+k}$ and forecasts of MACB_{n+k} and SDACB_{n+k} yield forecasts of $\gamma_{i,n+k}$; these are then combined via (4.4) with forecasts of TFR_{n+k} and $b_{i,n+k}$ to yield forecasts of the age-specific rates, $\hat{F}_{in}(k)$.

We now illustrate the roles of the gamma curve and bias forecasts in forecasting the fertility rates $F_{i,n+k}$. Figure 9a displays fertility rate data and the fitted gamma curve for 1982, compared with the 1980-origin forecasts of the data and gamma curves. The forecast curve (---) appears to predict accurately the fitted curve (—), but is less ac-

curate in forecasting the actual age-specific rates (\times). When the bias forecasts are added to the forecast gamma curve, the age-specific rate forecasts (o) are notably improved. In fact, the bias-adjusted forecasts for 1982 are almost uniformly better across age than the raw gamma curve forecasts.

From Figures 5 and 6, we see the 1980-origin MACB and SDACB forecasts undershoot the actual values by amounts that increase steadily from 1981 through 1984. This results in forecasted curves that peak too early and are too narrow. In Table 2 we give 1980-origin TFR forecasts, actual values, percentage forecast errors, and percentage forecast standard errors for 1981–1984. The TFR forecasts are accurate, so most of the error in forecasting the age-specific rates is due to the less accurate MACB and SDACB forecasts and errors in the bias forecasts.

The importance of bias adjustment decreases as forecast lead time increases. Table 2 shows that there is a larger error in forecasting TFR for 1983 and 1984 than in 1981 and 1982, and the MACB and SDACB forecasts are also less accurate in 1983–1984. Figure 9b shows that the 1984 curve forecast is less accurate than 1982. With the larger error in the curve forecast for 1984, bias adjustment makes less relative improvement. There is some improvement at specific ages, but the bias forecasts are most important in the short term (especially 1–2 years ahead). Bias adjustment is generally not important for longer-term forecasts (certainly beyond 10 years ahead), except perhaps at the very low and high ages.

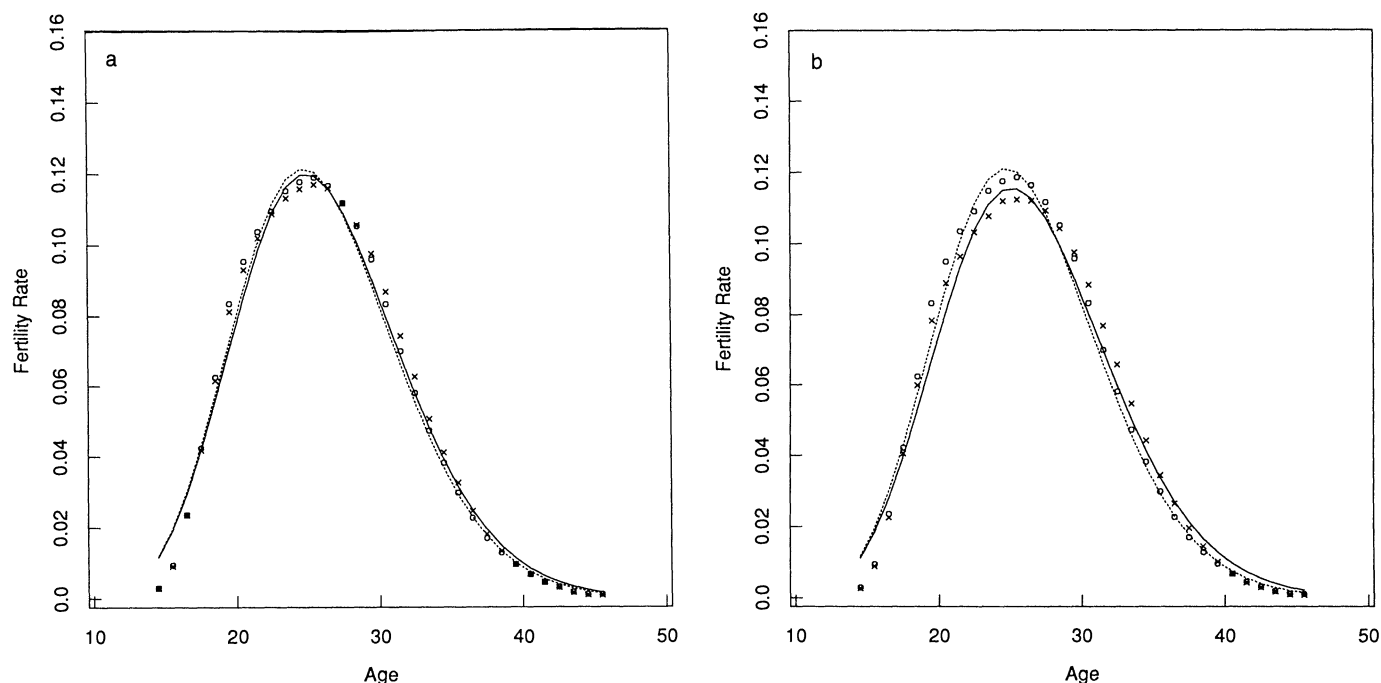


Figure 9. Actual and Forecasted Fertility Rates, and Fitted and Forecasted Gamma Curves: (a) 1982; (b) 1984. The curve parameters are forecast from 1980 using Model (3.1) estimated with data through 1980. The forecast parameters produce forecast gamma curves (---) that may be compared with the fitted gamma curves (—), obtained when the data for a given year become available. The forecasted curves are then "bias adjusted" (see text) to produce forecasts of age-specific fertility rates (o) that may be compared with the actual fertility rates (\times). The graphs show the importance of bias-adjusting the forecasted gamma curves in producing short-term, age-specific fertility rate forecasts. Note the adjustment is less effective in 1984, farther from the forecast origin.

Table 2. Accuracy Checks on 1980-Origin TFR Forecasts

Year	Forecast ^a	Actual	% Error ^b	Forecast % standard error ^c
1981	1.715	1.723	-.46%	2.9%
1982	1.720	1.730	-.58%	5.5%
1983	1.725	1.701	+1.41%	8.0%
1984	1.720	1.710	+.58%	10.8%

^a Computed as $\exp(\hat{T}_{1980}(k))$ for $k = 1, \dots, 4$ with $\hat{T}_{1980}(k)$ the forecasts computed from (4.2) with model parameters estimated using data through 1980.

^b Computed as $100(\text{forecast} - \text{actual})/\text{actual}$.

^c Computed as $100[\exp(v_{11}(k)^{1/2}) - 1]$ for $k = 1, \dots, 4$ with $v_{11}(k)$ the first diagonal element in (4.3), using the model parameters estimated with data through 1980.

5. IMPLEMENTATION IN CENSUS BUREAU POPULATION PROJECTIONS

In its latest set of national population projections, the Census Bureau projected fertility by combining short-term forecasts from time series models with long-term results based on demographic judgment. The TFR series modeled differs from ours in that $\ln(\text{TFR} - 1)$ was used instead of $\ln(\text{TFR})$ to prevent TFR forecasts and forecast limits from going below 1. A transfer function form similar to (3.3) was used to facilitate outlier detection and modification and to facilitate adjusting TFR forecasts for preliminary information available on 1985–1986 total births [this adjustment is described in Bell et al. (1988)]. The slightly different time series methods were presented here to simplify exposition. In what follows we describe how demographic judgment was used in conjunction with time series results, and we compare the Census Bureau projections with the results obtained directly from Model (3.1).

In the official Census Bureau projections, traditional judgmental methods were used to set the ultimate fertility level and mean age of childbearing for women completing their fertility after the year 2020. These were then compared with the fertility levels and mean ages from past cohorts to produce an assumed ultimate pattern of age-specific cohort fertility. Ultimate fertility forecasts may be obtained from Model (3.1), since the forecasts of all quantities needed (TFR, MACB, SDACB, and the biases) level off. As shown in Figure 10, the age distributions of fertility are roughly comparable for the two approaches, with the Census Bureau rates having a somewhat narrower and later peak, reflecting a lower SDACB and higher MACB.

The official projections used bias-adjusted forecasts from transfer function models for ages 14–39, through the first six years of the forecast period. These models, however, forecast increases in MACB and SDACB that produced increases in fertility to women 40 and over that, although small in absolute magnitude (Fig. 10), were large in percentage terms. Census Bureau demographers felt that they could not accept such rapid rises in fertility at these ages for the projections to have face validity, so the rates at these ages were forecast to remain constant at current levels. The results of this adjustment were inconsequential for the total birth and population projections, since the fertility rates above 40 are so small.

The differences between the Census Bureau projections

and Model (3.1) forecasts for the years 1985–1990 are due in part to use of different models. A greater difference is due to adjusting Census Bureau TFR forecasts for preliminary data on total births; forecasts were generated in late 1987, at which time preliminary estimates of the total number of 1985–1986 births, but not the age-specific distribution, were known. The effect of this adjustment can be seen in the 1985–1986 TFR numbers in Table 3.

The Census Bureau interpolated between the 1990 forecasts and the judgmentally determined ultimate values to get age-specific rates for the intermediate years. The Census Bureau-projected TFR, mean age of childbearing, and standard deviation of age at childbearing for 1985–1994, 2000, 2010, and 2020, and the Model (3.1) equivalents are in Table 3. In Table 3, both means and both standard deviations are computed empirically from the forecast age-specific relative fertility rates, \hat{R}_{it} , according to

$$\text{EMACB} = \sum_{i=14}^{45} \hat{R}_{it}(i + \frac{1}{2})$$

$$\text{ESDACB} = \left[\sum_{i=14}^{45} \hat{R}_{it}(i + \frac{1}{2} - \text{EMACB})^2 \right]^{1/2}. \quad (5.1)$$

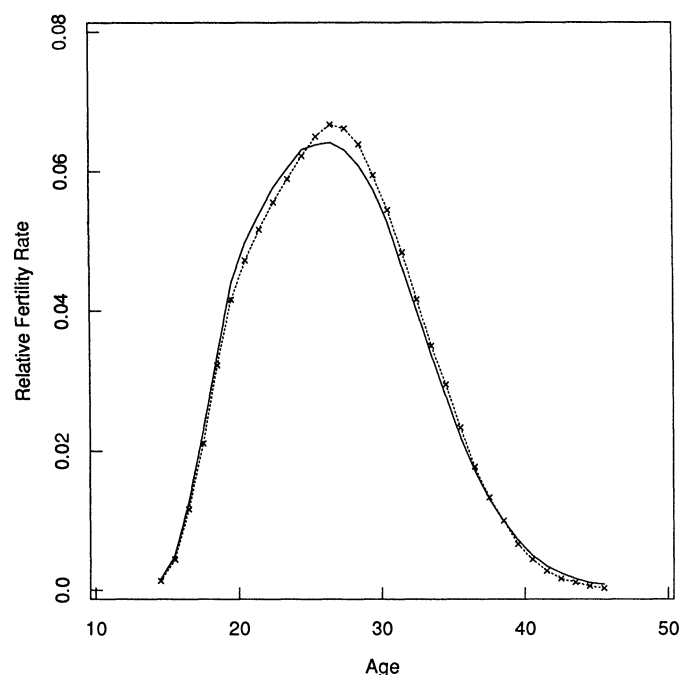


Figure 10. Ultimate Fertility Distributions, Census Projections (\times), and Forecasts From Model (3.1) (—). The graph compares the ultimate distribution of relative fertility rates from the U.S. Bureau of the Census (1988) projections to the distribution forecast from Model (3.1). The census-projections curve was determined judgmentally, as described in the text. The Model (3.1) curve was determined from bias-adjusted age-specific fertility rate forecasts using the gamma curve obtained from the ultimate forecasts of the curve parameters. The census projections show a slightly higher ultimate mean age and slightly lower ultimate standard deviation than those resulting from the model (see Table 3). Notice that the census projections for ages 40 and over are lower than the model forecasts. The census projections hold these relative rates at their 1984 values to avoid projecting an increase in fertility at these ages that is large in percentage terms though small in absolute magnitude.

Table 3. Model (3.1) Forecasts Compared With Census Bureau Projections of Total Fertility Rates (TFR) and Comparisons of Empirical Means and Standard Deviations of Age at Childbearing

Year	TFR		Mean age		Standard deviation	
	Census	Model	Census	Model	Census	Model
1984	1.710	1.710	26.51	26.51	5.52	5.52
1985	1.746	1.719	26.60	26.58	5.56	5.58
1986	1.747	1.714	26.66	26.63	5.58	5.63
1987	1.749	1.715	26.70	26.66	5.58	5.67
1988	1.769	1.717	26.73	26.69	5.58	5.69
1989	1.778	1.717	26.75	26.71	5.59	5.71
1990	1.781	1.717	26.78	26.72	5.60	5.73
1991	1.778	1.718	26.75	26.73	5.56	5.74
1992	1.778	1.718	26.76	26.74	5.56	5.74
1993	1.778	1.718	26.77	26.74	5.55	5.75
1994	1.779	1.718	26.78	26.74	5.55	5.75
1995	1.779	1.718	26.79	26.75	5.55	5.76
2000	1.780	1.718	26.83	26.75	5.54	5.76
2010	1.791	1.718	26.89	26.76	5.53	5.76
2020	1.800	1.718	26.92	26.76	5.54	5.76

NOTE: The figures for 1984, the last year of complete data, are shown for comparison. The Census Bureau TFR projections for 1985 and 1986 were adjusted for preliminary data on total births for those years. Both means and standard deviations of the age of childbearing are computed empirically, using text Equation (5.1), from the projected fertility distribution by age in each year.

Source: U.S. Bureau of the Census (1988) and unpublished data.

The TFR projections are within one-tenth of a child of the forecasts using Model (3.1), and the mean age and standard deviation projections do not differ greatly from the corresponding forecasts from Model (3.1). The projected mean age and standard deviation differ from the forecast gamma curve MACB and SDACB because of bias adjustment and because the gamma curve is continuous whereas the empirical calculations are discrete.

Time series methods were also used to aid in developing alternate high and low fertility variants of the projections by setting TFR projections at upper and lower 67% limits from a model for $\ln(\text{TFR} - 1)$ analogous to (3.3) for T_t . By 2020, the lower forecast limit for the total fertility rate in Model (3.1) reaches .78 and the upper limit reaches 3.78 (see Table 4). This three-child range is far wider than

the traditional one-child range between high and low series in judgmental demographic projections of U.S. fertility. This large range is indicative of the large amount of uncertainty inherent in forecasts that are based only on historical time series and does not take into account the substantive knowledge available to demographers.

Even though the forecasts do not differ greatly from the middle fertility series projected by demographic methods, demographers would be unlikely to accept the wide range between high and low fertility produced by time series models in the middle to long run. This is primarily because demographers contend that the large swings in fertility during the baby boom and bust of 1945–1974 were generated by a fertility process that is not likely to be repeated; the stability in fertility rates since 1974 has been cited to

Table 4. Census High, Middle, and Low Series of Total Fertility Rate Projections Compared With Model (3.1) Forecasts and 67% Intervals

Year	Census			Model (3.1)		
	Low series	Middle series	High series	Lower limit	Point forecast	Upper limit
1984		1.710			1.710	
1985		1.746		1.670	1.719	1.769
1986		1.747		1.626	1.714	1.806
1987	1.718	1.749	1.780	1.591	1.715	1.847
1988	1.716	1.769	1.826	1.554	1.717	1.898
1989	1.708	1.778	1.855	1.513	1.717	1.949
1990	1.689	1.781	1.885	1.473	1.717	2.001
1991	1.671	1.778	1.901	1.434	1.718	2.056
1992	1.662	1.778	1.916	1.396	1.718	2.113
1993	1.652	1.778	1.931	1.359	1.718	2.170
1994	1.642	1.779	1.946	1.324	1.718	2.229
1995	1.632	1.779	1.961	1.290	1.718	2.288
2000	1.583	1.780	2.035	1.140	1.718	2.588
2010	1.514	1.791	2.159	.924	1.718	3.192
2020	1.500	1.800	2.200	.780	1.718	3.784

NOTE: The figures for 1984, the last year of complete data, are shown for comparison. The Census Bureau TFR projections for 1985 and 1986 were adjusted for preliminary data on total births for those years. These are treated like actual data, which is why there are no low or high series Census Bureau projections for 1985–1986.

Source: U.S. Bureau of the Census (1988) and unpublished data.

support this argument. Consequently, in the Census Bureau projections the high and low fertility variants were constrained to 2.2 and 1.5, respectively (Table 4).

6. SUMMARY

We have presented an approach that accomplishes the goals of reducing dimensionality, providing short-term fertility forecasts of reasonable accuracy, and yielding long-term forecasts that capture the smooth shape across age of historical data. It allows the fertility forecaster to concentrate on modeling and predicting demographically meaningful quantities (TFR, MACB, and SDACB), since the gamma curves capture much of what is going on in the data. The deviations of the fitted curves from the age-specific rates can be forecast by simple techniques, and the forecasted curves can be adjusted accordingly. These bias adjustments are important for short-term accuracy, much less important in the long run.

In recent Census Bureau projections, short-term forecasts (through 1990) from a time series model similar to that presented here were combined with long-term projections from the judgmental approach described at the beginning of this article. Long-term forecasts by any method are likely to contain a substantial amount of error and so are perhaps best guided by judgment and substantive theory rather than by atheoretical time series forecasts. Hence the Census Bureau projections used the forecasted, bias-adjusted gamma curves for the first few years of the projection period and then interpolated between these and assumed ultimate levels determined by demographic theory.

[Received January 1987. Revised August 1988.]

REFERENCES

- Akaike, H. (1973), "Information Theory and an Extension of the Maximum Likelihood Principle," in *2nd International Symposium on Information Theory*, eds. B. N. Petrov and F. Csaki, Budapest: Akademiai Kiado, pp. 267–281.
- Bell, W. R., and Hillmer, S. C. (1983), "Modeling Time Series With Calendar Variations," *Journal of the American Statistical Association*, 78, 526–534.
- Bell, W. R., Long, J. F., Miller, R. B., and Thompson, P. A. (1988), "Multivariate Time Series Projections of Parameterized Age-Specific Fertility Rates," Research Report 88-16, U.S. Bureau of the Census, Statistical Research Division, Washington, DC.
- Carter, L. R., and Lee, R. D. (1986), "Joint Forecasts of U.S. Marital Fertility, Nuptiality, Births, and Marriages Using Time Series Models," *Journal of the American Statistical Association*, 81, 902–911.
- Coale, A. J., and Trussell, T. J. (1974), "Model Fertility Schedules: Variations in the Age Structure of Childbearing in Human Populations," *Population Index*, 40, 185–258.
- De Beer, J. (1985), "A Time Series Model for Cohort Data," *Journal of the American Statistical Association*, 80, 525–530.
- Hannan, E. J. (1970), *Multiple Time Series*, New York: John Wiley.
- Heuser, R. L. (1976), "Fertility Tables for Birth Cohorts by Color: United States, 1917–1973," Publication HRA 76-1152, U.S. Department of Health, Education, and Welfare, Washington, DC.
- Hoem, J. M., Madsen, D., Nielsen, J. L., and Ohlsen, E. (1981), "Experiments in Modelling Recent Danish Fertility Curves," *Demography*, 18, 231–244.
- Land, K. C. (1986), "Methods for National Population Forecasts: A Review," *Journal of the American Statistical Association*, 81, 888–901.
- Lee, R. D. (1974), "Forecasting Births in Post-Transitional Populations: Stochastic Renewal With Serial Correlated Fertility," *Journal of the American Statistical Association*, 69, 607–617.
- (1975), "Natural Fertility, Population Cycles, and the Spectral Analysis of Births and Marriages," *Journal of the American Statistical Association*, 70, 295–304.
- Long, J. F. (1981), Comment on "Modeling Demographic Relationships: An Analysis of Forecast Functions for Australian Births," by J. McDonald, *Journal of the American Statistical Association*, 76, 796–798.
- (1984), "U.S. National Population Projection Methods: A View From Four Forecasting Traditions," *Insurance: Mathematics and Economics*, 3, 231–239.
- McDonald, J. (1979), "A Time Series Approach to Forecast Australian Total Live Births," *Demography*, 16, 575–602.
- (1981), "Modeling Demographic Relationships: An Analysis of Forecast Functions for Australian Births," *Journal of the American Statistical Association*, 76, 782–792.
- Rao, C. R. (1965), *Linear Statistical Inference and Its Applications*, New York: John Wiley.
- Rogers, A. (1986), "Parameterized Multistate Population Dynamics and Projections," *Journal of the American Statistical Association*, 81, 48–61.
- Saboia, J. L. M. (1977), "Autoregressive Integrated Moving Average (ARIMA) Models for Birth Forecasting," *Journal of the American Statistical Association*, 72, 264–270.
- Tiao, G. C., and Box, G. E. P. (1981), "Modeling Multiple Time Series With Applications," *Journal of the American Statistical Association*, 76, 802–816.
- U.S. Bureau of the Census (1984), "Projections of the Population of the United States, by Age, Sex and Race: 1983–2080," Current Population Report 952 (Ser. P-25), Washington, DC: U.S. Government Printing Office.
- (1988), "Projections of the Population of the United States, by Age, Sex, and Race: 1988–2080," Current Population Report 1018 (Ser. P-25), Washington, DC: U.S. Government Printing Office.
- Whelpton, P. K. (1947), *Forecasts of the Population of the United States: 1945–1975*, Washington, DC: U.S. Bureau of the Census.
- Willekens, F. (1984), "An Age-Period-Cohort Model," unpublished paper presented at the annual meeting of the Population Association of America.